Title

Catalytic Dynamic Kinetic Resolutions in Tandem to Construct Two-Axis Terphenyl Atropisomers

Journal

Journal of the American Chemical Society, 142(38)

ISSN

0002-7863

Authors

Beleh, Omar M
Miller, Edward
Toste, F Dean
et al.

Publication Date

2020-09-23

DOI

10.1021/jacs.0c08057

Peer reviewed

HHS Public Access

Author manuscript

J Am Chem Soc. Author manuscript; available in PMC 2021 September 23.

Published in final edited form as:

J Am Chem Soc. 2020 September 23; 142(38): 16461–16470. doi:10.1021/jacs.0c08057.

Catalytic Dynamic Kinetic Resolutions in Tandem to Construct Two-Axis Terphenyl Atropisomers

Omar M. Beleh[†], **Edward Miller**[‡], **F. Dean Toste**[‡,*], **Scott J. Miller**[†,*]

[†]Department of Chemistry, Yale University, New Haven, Connecticut 06520, United States

[‡]Department of Chemistry, University of California, Berkeley, California 94720, United States

Abstract

The defined structure of molecules bearing multiple stereogenic axes is of increasing relevance to materials science, pharmaceuticals, and catalysis. However, catalytic enantioselective approaches to control multiple stereogenic axes remain synthetically challenging. We report the catalytic synthesis of two-axis terphenyl atropisomers, with complementary strategies to both chlorinated and brominated variants, formed with high diastereo- and enantioselectivity. The chemistry proceeds through a sequence of two distinct dynamic kinetic resolutions: first, an atroposelective ring-opening of Bringmann-type lactones produces a product with one established axis of chirality; second, a stereoselective arene halogenation delivers the product with the second axis of chirality established. In order to achieve these results, a class of Brønsted basic guanidinylated peptides, which catalyze an efficient atroposelective chlorination, is reported for the first time. In addition, a complementary bromination is reported, which also establishes the second stereogenic axis. These bromo-terphenyls are accessible following the discovery that chiral anion phase transfer catalysis by C_2-symmetric phosphoric acids allows catalyst control in the second stereochemistry-determining event. Accordingly, we established the fully catalyst-controlled stereodivergent synthesis of all possible chlorinated stereoisomers, while also demonstrating diastereodivergence in the brominated variants, with significant levels of enantioselectivity in both cases.

Graphical Abstract

[*]Corresponding Authors: scott.miller@yale.edu, fdtoste@berkeley.edu.

Supporting Information

The Supporting Information is available free of charge on the ACS Publications website.

Experimental details, characterization, and X-ray crystallographic data (PDF)

X-ray data for (*aS, aR*)-**4b** (CIF)

X-ray data for (*aR, aS*)-**4b** (CIF)

The authors declare no competing financial interests.

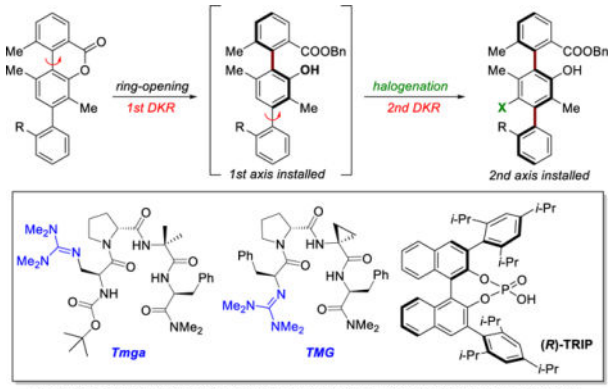

INTRODUCTION

Arising from hindered bond rotation, atropisomerism has become recognized as an important structural element within numerous chiral ligands, organocatalysts, and biologically active molecules. Tremendous strides have been made towards efficient and modular catalytic syntheses of single-axis atropisomers, especially in recent years.[1] Common strategies include stereoselective cross-coupling of two aryl units,[2] kinetic resolution of a pre-existing stereochemically undefined axis,[3–4] and atroposelective *de novo* construction of an arene ring.[5] However, application of these methods to multi-axis systems has only been recently explored.[6–19] These reports have often featured some of the established methods, including atroposelective cross-coupling,[7.13] [2+2+2]-cycloaddition,[8,10–11] or central-to-axial chirality transfer[15–16,18] to install two stereogenic axes at different sites of a substrate in a single step. This approach, which has many advantages, may also limit the modularity and scope of accessible multi-axis structures, especially in cases where different classes of reactions are required to allow differential functionalization in the vicinity of each stereogenic axis; moreover, a singular chemical reaction to set two axes with a common reaction may not be amenable to the development of diastereodivergent outcomes.

On the other hand, decoupling the individual steps and controlling the configuration of each chiral axis independently can offer a path to stereodivergency,[15,18] potentially through different chemical events at each axis. Achieving catalyst-control over all possible stereoisomers is challenging however, and can require extensive assessment of reaction conditions and multiple synthetic steps. Additionally, substrate-controlled stereoselectivity preferences must be addressed and overcome in molecules containing one or more stereochemical elements. Pioneering work in this area has come from the Sparr laboratory, which triumphantly demonstrated atroposelective aldol condensations to obtain products with high levels of atroposelectivity in systems possessing up to four fully controlled chiral axes in the oligonaphthalene template.[5a,15]

The approach we detail below describes a strategy to two-axis terphenyls based on catalytic dynamic kinetic resolution (DKR)[20] of starting materials that contain two configurationally labile axes. Rapid inter-conversion between two atropisomers at each axis through bond

rotation defines the challenge as a four-stereoisomer problem, and requires that each atroposelective reaction yield a configurationally stable axis (Fig 1a). The exploitation of this dynamic behavior was pioneered by Bringmann with biaryl lactones like **1**;[3] selective ring-opening of the lactone yields configurationally stable enantioenriched biaryls like **2**, as was elegantly demonstrated with a cinchona alkaloid-based catalyst by Wang (Fig 1b).[21–23] Our group[24] and others[3–4] have also previously utilized the concepts of catalytic atroposelective DKR, most relevantly in the bromination of phenol-containing biaryls promoted by a Brønsted basic dimethylaminoalanine (Dmaa) peptide (Fig 1c)[24a] Building on these precedents, we envisioned a two-event sequence by combining the two strategies that could access products with multiple configurationally stable axes. The key to this strategy is that atroposelective biaryl lactone ring-opening unveils a phenol, which is required for the next reaction, atroposelective electrophilic aromatic substitution. In order to test this hypothesis, we designed terphenyl lactone **3** (Fig 1d). In this proposed scenario, selective base-catalyzed alcoholysis of **3** yields enantioenriched *int*-**I**, which is then "turned on" for further functionalization, as the now revealed phenol enhances the reactivity of the *para*- position of the middle arene ring. An additional catalytic DKR through electrophilic halogenation of *int*-**I** installs the second stereogenic axis, yielding multi-axis atropisomers **4**. In addition to the fundamental interests presented by the terphenyl scaffold, these types of structures have proven to be of great interest to a number of applications, including as α-helix mime tics in medicinal chemistry[25] and as subunits in studies of oligoarene-based materials.[26]

RESULTS AND DISCUSSION

To establish a relevant catalytic atroposelective biaryl lactone ring-opening, we developed a new class of Brønsted basic guanidinylated peptides as catalysts for ring-opening of Bringmann-type lactones (Table 1). Notably, we were also mindful that Lewis basic catalysts of this type might also catalyze an asymmetric arene halogenation,[24,27] therefore possibly establishing the second chiral axis. Initially, we had hoped that Dmaa-based peptides, effective for enantioselective ring-openings of oxazolones through DKR,[28] and for arene halogenation,[24] would be effective in the selective conversion of **3** to **4**. However, these experiments were unsuccessful in attempted conversions of **1a** to **2a** (with **P1;** Table 1, entry 1), and in fact Et_3N was also ineffective as a catalyst (Table 1, entry 2). Anticipating that a more basic amine was required, we discovered that *N*,*N*,*N*',*N*'-tetramethylguamdine (**TMG**) was in fact a competent catalyst for the ring-opening (70% conv.; Table 1, entry 3), thus grounding our interest in TMG-based peptides as Brønsted basic catalysts.[29–31] Accordingly, we prepared a small set of tetramethylguanidinylalanine (Tmga)-containing peptides for evaluation in the enantioselective ring-opening of lactone **1a.** For this new family of guanidinylated peptide catalysts, we were motivated to focus on β-turn biased sequences,[32] as this type of secondary structure has proven successful in the past for mechanistically similar chemistry.[24,28]

Thus, through examination of such Brønsted basic guanidinylated sequences, we were pleased to find that the Tmga peptides could induce atroposelectivity *via* ring-opening with appreciable enantioselectivity, albeit at moderate conversion (**P2**, 74:26 er, 48% conv.; Table 1, entry 4). An evaluation of solvent effects included observations of enhanced conversion

and selectivity in polar, aprotic solvents (with **P2**, up to 87:13 er and up to 98% conv.; Table 1, entries 5–7, see Supporting Information for full details of the solvent effect studies) .We attribute these enhancements to the modulation of the guanidinium pK_a, as reflected in the acid-base equilibria between the peptide catalyst and the liberated phenol of **2** following ring-opening in the different solvents.[33] For example, in THF and MeCN, the phenolate is more basic, resulting in the major species at equilibrium to be the protonated phenol and guanidine free-base; this is the desired state of affairs to facilitate catalytic turnover. Further variation of the peptide sequence provided minor changes to er (see Supporting Information for details); however, improvements could be observed with an aryl group at the *i+3* position (**P3**, 91:9 er, **P4**, 90:10 er; Table 1, entries 8–9). Thus, we selected the sequence Boc-Tmga-D-Pro-Aib-Phe-Nme_2 (**P3**) for further optimization of reaction parameters. Increasing the reaction concentration, while lowering the temperature and equivalents of nucleophile improved enantioselectivity (93:7 er; Table 1, entry 10).

Also of note, we investigated the effect of substituents on the "lower" ring of biaryl lactone **1a.** In analogy to the observations of Wang,[22b] the highest enantioselectivity is observed when the position *ortho*- to the phenolic oxygen is substituted. In the present system, with catalyst **P3**, this appears to primarily be a steric effect; for example, permuting the *tert*-butyl group to a methyl substituent results in a small decrease of enantioselectivity (**1b**, 88:12 er; Table 1, entry 11). Removal of this group altogether (R = H) significantly lowers er (**1c**, 62:38 er, Table 1, entry 12). We believe that lactone ring-opening can be reversible under the basic conditions, leading to thermodynamic equilibration and racemization, which we observe when we resubmit **2c** to basic reaction conditions. Lactone **1a** is also vulnerable to these erosions, but more forcing conditions are required for complete racemization of **2a** (see Supporting Information for details).

With desirable ring-opening conditions in hand, we turned our attention to developing the targeted atroposelective halogenation to set the second axis. For this event, we were initially motivated to develop a novel atroposelective chlorination, despite the fact that atroposelective brominations were better precedented,[24] because the new Tmga catalysts provide enhanced Lewis basicity than the previously studied Dmaa-based catalysts. Atroposelective arene chlorinations have been historically slower to emerge, perhaps due to the lower reactivity of many conventional electrophilic chlorination reagents relative to the brominated counterparts [e.g. *N*-chlorosuccinimide (NCS) vs. *N*-bromosuccinimide (NBS)], [34–35] although enantioselective alkene chlorinations are well-known.[36] Introduction of aryl chlorides is also highly desirable due to their oft-noted pharmacological properties.[37] These issues, taken together, stimulated our pursuit of an atroposelective chlorination to establish the second axis, given our newfound access to the more active guanidinylated peptides.

We thus prepared terphenyl **3a**, and following lactone ring-opening, we investigated the catalytic viability of arene chlorination. Treatment of the resulting phenol with NCS in the absence of a catalyst resulted in only recovered starting material, establishing a minimal background rate (Table 2, entry l). However, in the presence of Tmga peptide **P3** the desired product **4a** was observed with full conversion, and with a 4.6:1 dr (Table 2, entry 2), confirming suitable catalytic activity. Parenthetically, a Dmaa-containing sequence that was previously optimized for bromination[24c] failed to catalyze the arene chlorination reaction

(**P1**; Table 2, entry 3). That said, guanidinylated catalyst **P3** provided only a minor enhancement of the intrinsic, substrate-controlled diastereoselectivity, since a similar result was obtained with an achiral guanidine base, triazabicyclodecene (**TBD**) (3.9:1 dr; Table 2, entry 4). A survey of a small set of Tmga-containing catalysts did not significantly perturb the diastereoselectivity beyond that observed with catalyst **P3** (See Supporting Information for details). However, we were pleased to observe that a related set of guanidinylated peptides, possessing the TMG moiety at the *N*-Terminus of the peptide sequence, was not only an excellent catalyst for chlorination, but also able to significantly influence the dr. Accordingly, after minimal optimization, we found that catalyst **P5** (TMG-Phe-D-Pro-Acpc-Phe-NMe_2) furnished **4a** cleanly in 13:1 dr and with 92:8 er for the major diastereomer (Table 2, entry 5). Abrief investigation of the peptide structure showed that the TMG-L-Phe-D-Pro stereochemistry was important for stereoselectivity (lower dr observed with **P6** and **P7;** Table 2, entries 6–7). The cyclopropyl ring of Acpc also at the *i*+2 position also conferred advantages, as its replacement with Aib led to a less selective catalyst (**P8**, Table 2, entry 8). Finally, lowering the catalyst loading of **P5** to 5 mol% (Table 2, entry 9) and addition of PhMe as a co-solvent provided improvements to 14:1 dr and 97:3 er for the major diastereomer (Table 2, entry 10).

Intriguingly, the er of **4a** is significantly enhanced relative to the simple ring-opened **2b** (97:3 er versus 88:12 er, respectively; compare Table 2 entry 10 to Table 1 entry 11). We ascribe this to a kinetic resolution of the intermediate chiral phenol (*int*-**I**, Fig. 1d). For the chlorination step, **P5** is well-matched with the major phenol (a*S*)-enantiomer and the reaction proceeds with excellent diastereoselectivity, favoring (a*S*,a*R*)-**4a** in over 50:1 dr (Scheme 1). Furthermore, the halogenation reaction of the minor phenol (a*R*) enantiomer with **P5** slightly favors the opposite diastereomer, (a*R*,a*R*)-**4a**, in 2:1 dr. This differential reactivity and distribution of products accounts for the overall enrichment of er — i.e., the increased ratio of (a*S*,a*R*)-**4a** to (a*R*,a*S*)-**4a** from the initial 88:12 er of **2b** attained after ring-opening.

We do wish to note parenthetically, it was not lost on us that since each DKR is promoted by a basic guanidine catalyst, a one-catalyst one-pot procedure might be possible, wherein a *singular guanidine-based catalyst might affect both atroposelective reactions, notably by a different reaction and distinct mechanism in each step.* Accordingly, we subjected lactone **3a** to the optimized ring-opening and chlorination sequence in a single pot with **P3**, which cleanly furnished **4a**, albeit with modest diastereoselectivity (3.5:1 dr, 88:12 er; Scheme 2a). This was not surprising, as **P3** alone was not particularly efficient in the chlorination event (as in Table 2, entry 1). We thus expected that an improved result could be obtained when the two guanidine-based catalysts **P3** and **P5** are present in one pot, as each peptide is optimized for each mechanistically distinct reaction. However, the situation is nuanced. When adding all catalysts and reagents immediately, we were surprised to see that reactivity was completely shut down (Scheme 2b). This may point to a guanidinium NCS complex rapidly forming in solution, which would diminish the basicity of the catalyst and thereby inhibit the ring-opening. Nonetheless, we found that addition of NCS only after formation of the ring-opened intermediate yielded **4a** in desirable levels of stereoselectivity (5.5:1 dr and 92:8 er for the major diastereomer; Scheme 2c). It is thus notable that good stereoselectivity

in chlorination is retained even with two catalyst sequences competing at differing efficiencies (compare Table 2, entry 1 vs. entry 10).

Returning to the optimized, sequential reaction conditions for establishing the synthesis of two-axis terphenyl products, we were interested in exploring the reaction scope. Therefore, we examined substituent effects on the efficiency and selectivity of the two-step sequence. Since an efficient DKR requires rapid isomerization of the second axis,[20] we tested the steric and electronic nature of the substituents on the bottom arene ring, which would directly influence the rate of bond rotation (Fig. 2). Lactone **3b** bearing an *ortho*- methoxy substituent, yielded the two-axis terphenyl **4b** in 72% yield, in 12:1 dr, and 97:3 er for the major diastereomer. Notably, no appreciable over-chlorination was detected in the electron-rich bottom arene ring. Chloro- (**3c**) and phenyl (**3d**) substituents are also well tolerated at the *ortho*- position, providing **4c** (9:1 dr, 95:5 er) and **4d** (7.7:1 dr, 99:1 er), respectively. However, sterically bulkier[38] substituents that may slow down aryl-aryl bond rotation eroded dr, as demonstrated by naphthyl-substituted **4e** (2.6:1 dr) and trifluoromethylated **4f** (1.5:1 dr). The er for both of these substrates was also lower (**4e**, 90:10 er; **4f**, 76:24 er). While we do not have a rock-solid explanation for the lower overall er for substrate **4f**, it is possible that inductive effects make this compound more acidic at the phenol, rendering racemization through reversible lactone and/or tetrahedral intermediate formation a vulnerability. Finally, the optimized conditions can be scaled successfully, albeit with slightly diminished yield. Performing the two-reaction sequence on 0.75 mmol (258 mg) of lactone **3b** furnished terphenyl **4b** in 53% overall yield (194 mg) in 14:1 dr and 97:3 er for the major diastereomer. We note that portion-wise addition of NCS was key to minimize the formation of overchlorinated byproducts (see Supporting Information for experimental details).

We now turn to the goal of fully stereodivergent conditions to achieve selective syntheses of all possible chlorinated terphenyl diastereomers. When developing a reaction system with multiple stereogenic elements, a catalyst might generally be optimized for one relative configuration of products (i.e. only one diastereomeric pair). Extensive reaction optimization and synthetic workarounds can be necessary to access the other diastereomers.[39] In the present case of setting two consecutive axes of chirality, when each axis is set by a different reaction (and thus differing reaction mechanisms), there exists a requirement for catalyst control, and any substrate-controlled selectivity biases must be identified and overcome.

Throughout our studies of the terphenyl system **3**, we observed that **P5** reacts primarily with the (a*S*)-enantiomer of the ring-opened intermediate *int*-**I** in high efficiency (as in Scheme 1), and as such we expected *ent*-**P5** to be matched with the (a*R*)-enantiomer. Thus, we envisioned utilizing the enantiomers of **P3** and **P5** in each possible combination, as these matched/mismatched effects of substrate and catalyst might overturn the intrinsic diastereoselectivity and achieve stereodivergency. We selected methoxy-substituted **3b** to assess this hypothesis. As a benchmark for the intrinsic diastereoselectivity, we determined that **3b** is converted to **4b** in the **TBD**-catalyzed chlorination with a 6:1 dr (favoring (a*S*,a*R*)-**4b** from (a*S*)-ring-opened product of type *int*-**I**; see Supporting Information for details). In the substrate-catalyst matched scenarios, treatment of **3b** with catalysts **P3** and **P5**, yielded (a*S*,a*R*)-**4b** (72% yield, 12:1 dr, 97:3 er; Scheme 3, top right). By analogy, treatment of **3b** with *ent*-**P3** and *ent*-**P5** delivered (a*R*,a*S*)-**4b** (Scheme 3, bottom left), in

72% yield, 12:1 dr, and 97:3 er, reflecting a high level of reproducibility. These results represent an overall enhancement of the intrinsic substrate-controlled diastereoselectivity. Furthermore, the substrate-catalyst mismatched cases successfully overturn the substrate-controlled diastereoselectivity observed with achiral base **TBD**. With catalysts **P3** and *ent*-**P5**, the intrinsically disfavored product (a*S*,a*S*)-**4b** is now the major diastereomer formed, and it is observed with very high enantioselectivity (2.5:1 dr, 99:1 er, in 60% yield; Scheme 3, top left). Finally, with catalysts *ent*-**P3** and **P5**, product (a*R*,a*R*)-**4b** is isolated in 55% yield, with a 2.7:1 dr and with 99:1 er (Scheme 3, bottom right; we ascribe the small difference in dr for the two cases to variable levels of conversion). The absolute and relative configurations for the series were unambiguously determined by X-ray crystallography. To further highlight the utility of this approach, each of the four diastereomers could be purified chromatographically to stereochemical homogeneity.

In parallel to the above studies on atroposelective chlorination to set the second stereogenic axis, we also wished to develop a complementary bromination, in line with previous studies of atroposelective arene brominations.[24] Initial evaluation of a few guanidine-based catalysts that are the focus of the present study with common electrophilic brominating reagents (namely *N*-bromosuccinimide and *N*-bromophthalimide) did not deliver dramatic nor improved dr and er values for brominated terphenyls of type *Br*-**4** (generally under 5:1 dr and no higher than 88:12 er). In contrast, an entirely different approach for the bromination step led to significantly better results right away. Predicated on chiral anion phase-transfer (CAPT) and C_2-symmetric chiral phosphoric acid-derived counter-ions, this strategy had been successfully applied to a variety of asymmetric halogenation reactions.[40] We posited this strategy could be well-suited for the bromination step to deliver *Br*-**4a** with stereodivergency. The approach also brings the advantage of low background reactivity in analogy to conventional chlorination chemistry - the brominating reagent is an insoluble solid, effectively isolating it from the substrate in solution. Thus, the brominating reagent only comes into solution upon salt metathesis with the phosphate anion catalyst, resulting in a soluble chiral ion pair and initiating reactivity. Moreover, we were stimulated by the success of Akiyama in applying C_2-symmetric chiral phosphoric acid catalysts to atroposelective biaryl desymmetrizations with conventional electrophilic halogenating reagents.[41]

The CAPT strategy thus examined the efficacy of DABCOnium salts as brominating reagents in terphenyl system **3**. Building on the utility of these reagents in the enantioselective bromocyclization of difluoroalkenes,[42] we surmised that analogous conditions could be directly applied to atroposelective electrophilic bromination of phenols. Notably, these DABCOnium-based reagents provided an additional parameter to optimize the stereoselectivity of the bromination event. A screen of several distinct salts revealed that $[(DAB)_2Br(BF_4)_3]$ (Scheme 4, abbreviated as $[Br]^+$) was a judicious choice for catalyst-controlled modulation of diastereoselectivity (see Supporting Information for details). Thus, following the **P3**-catalyzed ring-opening of **3a**, we treated the unpurified intermediate with (*S*)-TRIP (10 mol%) as the phase transfer catalyst and DABCOnium salt $[(DAB)_2Br(BF_4)3]$, which delivered the two axis terphenyl product *Br*-**4a** in 60% yield, 2.5:1 dr, and with excellent enantioenrichment (98:2 er; Scheme 4a, to the right). We again attribute this

overall enhancement in er to the differential functionalization rates of the enantiomers of the ring-opened phenol, in analogy to the kinetic resolution process described in Scheme 1. Strikingly, and in line with our goals, the diastereoselectivity can be overturned by swapping the chirality of the phase transfer catalyst. Employing (*R*)-TRIP in the bromination step affords *Br*-**4a'** in 82% yield, 6.8:1 dr, and in excellent enantiopurity (99:1 er; Scheme 4a, to the left). We also assessed the CAPT strategy on substrates that performed less efficiently in chlorination. Importantly, subjecting 2-naphthyl-substituted lactone **3e** to the same ring-opening and bromination sequence with (*S*)-TRIP as the phase transfer catalyst yielded *Br*-**4e** in 64% yield, with 1.4:1 dr and improved enantioselectivity of relative to the chlorinated variant (94:6 er; Scheme 4b, to the right). As with *Br*-**4a**, diastereodivergence could be achieved by swapping the stereochemistry of the catalyst to (*R*)-TRIP, furnishing the opposite diastereomer *Br*-**4e'** in 83% yield, albeit with a modest 3.7:1 dr, but with excellent enantioenrichment (98:2 er; Scheme 4b, to the left). Despite the clear mechanistic differences between the chlorination and bromination reactions, they are complementary in allowing stereodivergent access to either chlorinated or brominated products, offering access to all stereoisomers of linear terphenyls of type **4**, and with excellent enantiopurity throughout the series.

CONCLUSIONS

In summary, we report conditions to synthesize two-axis atropisomers with access to all possible diastereomers with catalyst control. We demonstrated complementary approaches to chlorinated and brominated terphenyls in excellent enantiopurity. In our studies, we developed a new class of strongly Brønsted basic guanidine peptide catalysts, which can be useful in targeting challenging transformations, such as the ring-opening and chlorination described in this work. As these two distinct reactions are both catalyzed by the guanidine moiety, we also established the possibility that a unique catalyst can afford appreciable levels of control for these two mechanistically distinct reactions in this sequence. Alongside these studies on chlorination, we established conditions for an atroposelective phosphoric acid-catalyzed diastereodivergent bromination through the CAPT strategy. In both the peptidyl guanidine-catalyzed reactions, and in the C_2-symmetric phosphoric acid-catalyzed reactions, not only were high levels of enantioselectivity achieved, but both catalytic approaches were found to be capable of overcoming and reversing the intrinsic, substrate-controlled diastereoselectivity. Taken together, this combination of approaches accomplishes comprehensive and controlled stereodivergent access to all possible diastereomers of the targeted terphenyl scaffolds. The catalyst-controlled, stereodivergent synthesis of multi-axis atropisomers remains a challenging endeavor, but seems likely to increase in importance as capabilities grow, and as appreciation of their properties expands in interdisciplinary contexts.

Supplementary Material

Refer to Web version on PubMed Central for supplementary material.

ACKNOWLEDGMENTS

F.D.T., and S.J.M. are grateful to the National Institute of General Medical Sciences of the National Institutes of Health for support (R01-121383). FDT acknowledges the NIH/NIGMS through grant R35-GM118190. SJM also acknowledges the NIH/NIGMS through grant R35-132092. We would like to thank Dr. Byoungmoo Kim, Dr. Margaret J. Hilton, and Dr. Hyung Yoon for their insight. We would also like to thank Dr. Brandon Q. Mercado for solving our X-ray crystal structures.

REFERENCES

(1). For selected reviews see(a)Bringmann G; Price Mortimer AJ; Keller PA; Gresser MJ; Garner J; Breuning M Atroposelective Synthesis of Axially Chiral Biaryl Compounds. Angew. Chem., Int. Ed 2005, 44, 5384–5427.(b)Bringmann G; Gulder T; Gulder TAM; Breuning M Atroposelective Total Synthesis of Axially Chiral Biaryl Natural Products. Chem. Rev 2011, 111, 563–639. [PubMed: 20939606] (c)Ma G; Sibi MP Catalytic Kinetic Resolution of Biaryl Compounds Chem. Eur. J 2015, 21, 11644–11657. [PubMed: 26237330] (d)Wencel-Delord J; Panossian A; Leroux FR; Colobert F Recent Advances and New Concepts for the Synthesis of Axially Stereoenriched Biaryls. Chem. Soc. Rev 2015, 44, 3418–3430. [PubMed: 25904287] (e)Renzi P Organocatalytic Synthesis of Axially Chiral Atropisomers. Org. Biomol. Chem 2017, 15, 4506–4516. [PubMed: 28497829] (f)Zilate B; Castrogiovanni A; Sparr C Catalyst-Controlled Stereoselective Synthesis of Atropisomers. ACS Catal. 2018, 8, 2981–2988.(g)Wang YB; Tan B Construction of Axially Chiral Compounds via Asymmetric Organocatalysis. Acc. Chem. Res 2018, 51, 534–547. [PubMed: 29419282] (h)Metrano AJ; Miller SJ Peptide-Based Catalysts Reach the Outer Sphere through Remote Desymmetrization and Atroposelectivity. Acc. Chem. Res 2019, 52, 199–215. [PubMed: 30525436] (i)Ros A; Ramírez P; Fernández R; Lassaletta JM Asymmetric Synthesis of Axially Chiral Biaryls and Heterobiaryls. Chapter 1. in Atropisomerism and Axial Chirality; World Scientific Publishing Co.: NJ, 2019.

(2). (a)Brussee J; Jansen ACA A Highly Stereoselective Synthesis of S(-)-[1,1'-Binaphthalene]-2,2'-Diol. Tetrahedron Lett. 1983, 24, 3261–3262.(b)Lloyd-Williams P; Giralt E Atropisomerism, biphenyls and the Suzuki coupling: peptide antibiotics. Chem. Soc. Rev 2001, 30, 145–157. (c)Hassan J; Sevignon M; Gozzi C; Schulz E; Lemaire M Aryl-aryl bond formation one century after the discovery of the Ullmann reaction. Chem. Rev 2002, 102, 1359–1469. [PubMed: 11996540] (d)Liao G; Zhou T; Yao QJ; Shi BF Recent advances in the synthesis of axially chiral biaryls via transition metal-catalysed asymmetric C–H functionalization. Chem. Comm 2019, 55, 8514–8523. [PubMed: 31276136] (e)Shen D; Xu Y; Shi S A Bulky Chiral N-Heterocyclic Carbene Palladium Catalyst Enables Highly Enantioselective Suzuki-Miyaura Cross-Coupling Reactions for the Synthesis of Biaryl Atropisomers. J. Am. Chem. Soc 2019, 141, 14938–14945. [PubMed: 31460761] (f)Nguyen QH; Guo SM; Royal T; Baudoin O; Cramer N, Intermolecular Palladium(0)-Catalyzed Atropo-enantioselective C–H Arylation of Heteroarenes. J. Am. Chem. Soc 2020, 142, 2161–2167.

(3). (a)Bringmann G; Breuning M; Tasler S The lactone concept: an efficient pathway to axially chiral natural products and useful reagents Synthesis. 1999, 4, 525–558.(b)Bringmann G; Breuning M; Pfeifer RM; Schenk WA; Kamikawa K; Uemura M The lactone concept—a novel approach to the metal-assisted atroposelective construction of axially chiral biaryl systems. J. Organomet. Chem 2002,661,31–47.(c)Bringmann G; Tasler S; Pfeifer RM; Breuning M The directed synthesis of axially chiral ligands, reagents, catalysts, and natural products through the lactone methodology J. Organomet. Chem 2002, 661,49–65.

(4). Selected examples:(a)Kakiuchi F; Le Gendre P; Yamada A; Ohtaki H; Murai S Atropselective alkylation of biaryl compounds by means of transition metal-catalyzed C–H/olefin coupling. Tetrahedron: Asymmetry 2000, 11, 2647–2651.(b)Miyaji R; Asano K; Matsubara S Bifunctional Organocatalysts for the Enantioselective Synthesis of Axially Chiral Isoquinoline N-Oxides. J. Am. Chem. Soc 2015, 137, 6766–6769. [PubMed: 26000800] (c)Jolliffe JD; Armstrong RJ; Smith MD Catalytic enantioselective synthesis of atropisomeric biaryls by a cation-directed O-alkylation. Nat. Chem 2017, 9, 558–562. [PubMed: 28537599]

(5). (a)Link A; Sparr C Organocatalytic Atroposelective Aldol Condensation: Synthesis of Axially Chiral Biaryls by Arene Formation. Angew. Chem., Int. Ed 2014, 53, 5458–5461.(b)Chen YH; Cheng DJ; Zhang J; Wang Y; Liu XY; Tan B Atroposelective Synthesis of Axially Chiral

Biaryldiols via Organocatalytic Arylation of 2-Naphthols. J. Am. Chem. Soc 2015, 137, 15062–15065. [PubMed: 26560999] (c)Moliterno M; Cari R; Puglisi A; Antenucci A; Sperandio C; Moretti E; Di Sabato A; Salvio R; Bella M, Quinine-Catalyzed Asymmetric Synthesis of 2,2 '-Binaphthol-Type Biaryls under Mild Reaction Conditions. Angew. Chem., Int. Ed 2016, 55, 6525–6529.(d)Kwon Y; Li JQ; Reid JP; Crawford JM; Jacob R; Sigman MS; Toste FD; Miller SJ, Disparate Catalytic Scaffolds for Atroposelective Cyclodehydration. J. Am. Chem. Soc 2019, 141, 6698–6705. [PubMed: 30920223] (e)Coombs G; Sak MH; Miller SJ, Peptide-Catalyzed Fragment Couplings that Form Axially Chiral Non-C_2-Symmetric Biaryls. Angew. Chem., Int. Ed 2020, 59, 2875–2880.

(6). For a recent review see:Bao X; Rodriguez J; Bonne D Enantioselective Synthesis of Atropisomers with Multiple Stereogenic Axes. Angew. Chem., Int. Ed 2020, 59, 12623–12634

(7). Hayashi T; Hayashizaki K; Ito Y Asymmetric Synthesis of Axially Chiral 1,1′:5′,1″- and 1,1′:4′,1″-Ternaphthalenes by Asymmetric cross-coupling with a Chiral Ferrocenylphosphine-nickel catalyst. Tetrahedron Lett. 1989, 30, 215–218.

(8). Shibata T; Fujimoto T; Yokota K; Takagi K Iridium complex-catalyzed highly enantio- and diastereoselective [2+2+2] cycloaddition for the synthesis of axially chiral teraryl compounds. J. Am. Chem. Soc 2004, 126, 8382–8383. [PubMed: 15237987]

(9). (a)Tsubaki K Synthesis and properties of the chiral oligonaphthalenes *Org*. Biomol. Chem 2007, 5, 2179–2188.(b)Takaishi K; Kawamoto M; Tsubaki K Multibridged chiral naphthalene oligomers with continuous extreme-cisoid conformation. Org. Lett 2010, 12, 1832–1835. [PubMed: 20337457]

(10). Oppenheimer J; Hsung RP; Figueroa R; Johnson WL Stereochemical control of both C–C and C–N axial chirality in the synthesis of chiral *N,O*-biaryls. Org. Lett 2007, 9, 3969–3972. [PubMed: 17764192]

(11). Tanaka K; Suda T; Noguchi K; Hirano M Catalytic [2 + 2 + 2] and Thermal [4 + 2] Cycloaddition of 1,2-Bis(arylpropiolyl)benzenes. J. Org. Chem 2007, 72, 2243–2246. [PubMed: 17288481]

(12). Barrett KT; Metrano AJ; Rablen PR; Miller SJ Spontaneous transfer of chirality in an atropisomerically enriched two-axis system. Nature 2014, 509, 71–75. [PubMed: 24747399]

(13). Dherbassy Q; Djukic JP; Wencel-Delord J; Colobert F Two stereoinduction events in one C–H activation step: A route towards terphenyl ligands with two atropisomeric axes. Angew. Chem., Int. Ed 2018, 57, 4668–4672.

(14). Tan Y; Jia S; Hu F; Liu Y; Peng L; Li D; Yan H Enantioselective Construction of Vicinal Diaxial Styrenes and Multiaxis System via Organocatalysis. J. Am. Chem. Soc 2018, 140, 16893–16898; [PubMed: 30463406]

(15). Lotter D; Castrogiovanni A; Neuburger M; Sparr C Catalyst-Controlled Stereodivergent Synthesis of Atropisomeric Multiaxis Systems. ACS Cent. Sci, 2018, 4, 656–660. [PubMed: 29806013]

(16). Hu Y-L; Wang Z; Yang H; Chen J; Wu Z-B; Lei Y; Zhou L Conversion of two stereocenters to one or two chiral axes: atroposelective synthesis of 2,3-diarylbenzoindoles. Chem. Sci 2019, 10, 6777–6784. [PubMed: 31391898]

(17). Jia S; Li S; Liu Y; Qin W; Yan H Enantioselective Control of Both Helical and Axial Stereogenic Elements though an Organocatalytic Approach. Angew. Chem. Int. Ed 2019, 58, 18496–18501.

(18). Bao X; Rodriguez J; Bonne D Bidirectional enantioselective synthesis of bis-benzofuran atropisomeric oligoarenes featuring two distal C–C stereogenic axes. Chem. Sci 2020, 11, 403–408.

(19). Takano H; Shiozawa N; Imai Y; Kanyiva KS; Shibata T Catalytic Enantioselective Synthesis of Axially Chiral Polycyclic Aromatic Hydrocarbons (PAHs) via Regioselective C–C Bond Activation of Biphenylenes. J. Am. Chem. Soc 2020, 142, 4714–4722.

(20). For selected reviews on DKR see:Noyori R; Tokunaga M; Kitamura M Stereoselective Organic Synthesis via Dynamic Kinetic Resolution. Bull. Chem. Soc. Jpn 1995, 68, 36–55.(b)Huerta FF; Minidis ABE; Backvall JE Racemisation in asymmetric synthesis. Dynamic kinetic resolution and related processes in enzyme and metal catalysis. Chem. Soc. Rev 2001, 30, 321–331. (c)Pellissier H Organocatalyzed Dynamic Kinetic Resolution. Adv. Synth. Catal 2011,353, 659–676.

(21). Selected examples:(a)Bringmann G; Hartung T First Atropo-Enantioselective Ring Opening of Achiral Biaryls Containing Lactone Bridges with Chiral Hydride-Transfer Reagents Derived from Borane. Angew. Chem., Int. Ed. Engl 1992, 31, 761–762.(b)Bringmann G; Hartung T Atropo-enantioselective biaryl synthesis by stereocontrolled cleavage of configuratively labile lactone-bridged precursors using chiral H-nucleophiles. Tetrahedron 1993, 49, 7891–7902. (c)Bringmann G; Breuning M; Walter R; Wuzik A; Peters K; Peters E-M Synthesis of Axially Chiral Biaryls by Atropo-Diastereoselective Cleavage of Configurationally Unstable Biaryl Lactones with Menthol-Derived O-Nucleophiles. Eur. J. Org. Chem 1999, 3047–3055.

(22). Selected examples:(a)Ashizawa T; Tanaka S; Yamada T Catalytic atropo-enantioselective reduction of biaryl lactones to axially chiral biaryl compounds. Org. Lett 2008, 10, 2521–2524. [PubMed: 18503278] (b)Yu CG; Huang H; Li XM; Zhang YT; Wang W Dynamic Kinetic Resolution of Biaryl Lactones via a Chiral Bifunctional Amine Thiourea-Catalyzed Highly Atropoenantioselective Transesterification. J. Am. Chem. Soc 2016, 138, 6956–6959. [PubMed: 27218264] (c)Mori K; Itakura T; Akiyama T Enantiodivergent Atroposelective Synthesis of Chiral Biaryls by Asymmetric Transfer Hydrogenation: Chiral Phosphoric Acid Catalyzed Dynamic Kinetic Resolution. Angew. Chem., Int. Ed 2016, 55, 11642–11646.

(23). Bringmann G; Menche D Stereoselective Total Synthesis of Axially Chiral Natural Products via Biaryl Lactones. Acc. Chem. Res 2001, 34, 615–624. [PubMed: 11513568]

(24). (a)Gustafson JL; Lim D; Miller SJ Dynamic Kinetic Resolution of Biaryl Atropisomers via Peptide-Catalyzed Asymmetric Bromination. Science, 2010, 328, 1251–1255. [PubMed: 20522769] (b)Barrett KT; Miller SJ Enantioselective Synthesis of Atropisomeric Benzamides through Peptide-Catalyzed Bromination. J. Am. Chem. Soc 2013, 135, 2963–2966. [PubMed: 23410090] (c)Diener ME; Metrano AJ; Kusano S; Miller SJ, Enantioselective Synthesis of 3-Arylquinazolin-4(3H)-ones via Peptide-Catalyzed Atroposelective Bromination. J. Am. Chem. Soc 2015, 137, 12369–12377. [PubMed: 26343278] (d)Metrano AJ; Abascal NC; Mercado BQ; Paulson EK, Miller SJ Structural Studies of β-Turn-Containing Peptide Catalysts for Atroposelective Quinazolinone Bromination. Chem. Commun 2016, 52, 4816–4819.

(25). (a)Yin H; Lee GI; Sedey KA; Kutzki O; Park HS; Orner BP; Ernst JT; Wang HG; Sebti SM; Hamilton AD Terphenyl-based bak BH3 α-helical proteomimetics as low-molecular-weight antagonists of Bcl-X-L J. Am. Chem. Soc 2005, 127, 10191–10196.(b)Yin H; Lee GI; Park HS; Payne GA; Rodriguez JM; Sebti SM; Hamilton AD Terphenyl-based helical mimetics that disrupt the p53/HDM2 interaction. Angew. Chem., Int. Ed 2005, 44, 2704–2707.

(26). Moerner WE Single-Molecule Spectroscopy, Imaging, and Photo-control: Foundations for Super-Resolution Microscopy (Nobel Lecture) Angew. Chem., Int. Ed 2015, 54, 8067–8093.

(27). Denmark SE; Burk MT Lewis base catalysis of bromo- and iodolactonization and cycloetherification. Proc. Nat. Acad. Sci 2010, 107, 20655–20660. [PubMed: 20705900]

(28). Metrano AJ; Miller SJ Peptide-Catalyzed Conversion of Racemic Oxazol-5(4H)-ones into Enantiomerically Enriched α-Amino Acid Derivatives. J. Org. Chem, 2014, 79, 1542–1554. [PubMed: 24517453]

(29). Selected reviews on chiral guanidines as catalysts, and references therein:(a)Leow D; Tan CH Chiral Guanidine Catalyzed Enantioselective Reactions. Chem. Asian J 2009, 4, 488–507. [PubMed: 19101939] (b)Selig P Guanidine organocatalysis. Synthesis 2013, 45, 703–718. (c)Hosoya K; Odagi M; Nagasawa K Guanidine organocatalysis for enantioselective carbon-heteroatom bond-forming reactions. Tetrahedron Lett. 2018, 59, 687–696.(d)Dong S; Feng X; Liu X Chiral Guanidines and Their Derivatives in Asymmetric Synthesis. Chem. Soc. Rev 2018, 47, 8525–8540. [PubMed: 30375584] (e)Chou HC; Leow D; Tan CH Recent Advances in Chiral Guanidine-Catalyzed Enantioselective Reactions. Chem. Asian J 2019, 14, 3803–3822. [PubMed: 31562680]

(30). Selected examples of chiral guanidines as Bronsted basic catalysts:(a)Isobe T; Fukuda K; Araki Y; Ishikawa T Modified guanidines as chiral superbases: the first example of asymmetric silylation of secondary alcohols. Chem. Commun 2001, 3, 243–244.(b)Ishikawa T; Araki Y; Kumamoto T; Seki H; Fukuda K; Isobe T Modified guanidines as chiral superbases: application to asymmetric Michael reaction of glycine imine with acrylate or its related compounds. Chem. Commun 2001, 3, 245–246.(c)Terada M; Ube H; Yaguchi Y Axially chiral guanidine as enantioselective base catalyst for 1,4-addition reaction of 1,3-dicarbonyl compounds with conjugated nitroalkenes. J. Am. Chem. Soc 2006, 128, 1454–1455. [PubMed: 16448108]

(d)Terada M; Nakano M; Ube H Axially chiral guanidine as highly active and enantioselective catalyst for electrophilic amination of unsymmetrically substituted 1,3-dicarbonyl compounds. J. Am. Chem. Soc 2006, 128, 16044–16045. [PubMed: 17165751] (e)Yu ZP; Liu XH; Zhou L; Lin LL; Feng XM Bifunctional Guanidine via an Amino Amide Skeleton for Asymmetric Michael Reactions of β-Ketoesters with Nitroolefins: A Concise Synthesis of Bicyclic β-Amino Acids. Angew.Chem. Int. Ed 2009, 48, 5195–5198.(f)Dong SX; Liu XH; Chen XH; Mei F; Zhang YL; Gao B; Lin LL; Feng XM Chiral Bisguanidine-Catalyzed Inverse-Electron-Demand Hetero-Diels-Alder Reaction of Chalcones with Azlactones. J. Am. Chem. Soc 2010, 132, 10650–10651. [PubMed: 20681686]

(31). Our group has previously studied guanidinylated peptides as chiral ligands in Cu-catalyzed cross-coupling. See:(a)Kim B; Chinn AJ; Fandrick DR; Senanayake CH; Singer RA; Miller SJ Distal Stereocontrol Using Guanidinylated Peptides as Multifunctional Ligands: Desymmetrization of Diarylmethanes via Ullman Cross-Coupling. J. Am. Chem. Soc 2016, 138, 7939–7945. [PubMed: 27254785] (b)Chinn AJ; Kim B; Kwon Y; Miller SJ Enantioselective Intermolecular C–O Bond Formation in the Desymmetrization of Diarylmethines Employing a Guanidinylated Peptide-Based Catalyst. J. Am. Chem. Soc 2017, 139, 18107–18114. [PubMed: 29116792] (c)Kwon Y; Chinn A; Kim B; Miller SJ Divergent Control of Point and Axial Stereogenicity: Catalytic Enantioselective C–N Bond Forming Cross-Coupling and Catalyst-Controlled Atroposelective Cyclodehydration. Angew. Chem., Int. Ed 2018, 57, 6251–6255.

(32). Metrano AJ; Abascal NC; Mercado BQ; Paulson EK; Hurtley AE; Miller SJ Diversity of Secondary Structure in Catalytic Peptides with β-Turn-Biased Sequences *J.* Am. Chem. Soc 2017, 139, 492–516.

(33). (a)Eckert F; Leito I; Kaljurand I; Kutt A; Klamt A; Diedenhofen M, Prediction of Acidity in Acetonitrile Solution with COSMO-RS. J. Comput. Chem 2009, 30, 799–810. [PubMed: 18727157] (b)Muckerman JT; Skone JH; Ning M; Wasada-Tsutsui Y, Toward the accurate calculation of pKa values in water and acetonitrile. Bba-Bioenergetics 2013, 1827, 882–891. [PubMed: 23567870] (c)Raamat E; Kaupmees K; Ovsjannikov G; Trummal A; Kutt A; Saame J; Koppel I; Kaljurand I; Lipping L; Rodima T; Pihl V; Koppel IA; Leito I, Acidities of strong neutral Bronsted acids in different media. J. Phys. Org. Chem 2013, 26, 162–170.(d)Himmel D; Radtke V; Butschke B; Krossing I, Basic Remarks on Acidity. Angew. Chem., Int. Ed 2018, 57, 4386–4411.(e)Tshepelevitsh S; Kutt A; Lokov M; Kaljurand I; Saame J; Heering A; Plieger PG; Vianello R; Leito I On the Basicity of Organic Bases in Different Media. Eur. J. Org. Chem 2019, 6735–6748.

(34). Golebiewski WM; Gucma M Applications of *N*-chlorosuccinimide in organic synthesis. Synthesis 2007, 23, 3599–3619.

(35). For a recent example employing guanidines as electrophilic chlorinating reagents see:Rodriguez RA; Pan CM; Yabe Y; Kawamata Y; Eastgate MD; Baran PS Palau'chlor: A Practical and Reactive Chlorinating Reagent. J. Am. Chem. Soc 2014, 136, 6908–6911. [PubMed: 24758725]

(36). Selected examples and references therein:(a)Whitehead DC; Yousefi R; Jaganathan A; Borhan B An Organocatalytic Asymmetric Chlorolactonization. J. Am. Chem. Soc 2010, 132, 3298–3300. [PubMed: 20170118] (b)Nicolaou KC; Simmons NL; Ying YC; Heretsch PM; Chen JS, Enantioselective Dichlorination of Allylic Alcohols. J. Am. Chem. Soc 2011, 133, 8134–8137. [PubMed: 21542622] (c)Cresswell AJ; Eey STC; Denmark SE, Catalytic, Stereoselective Dihalogenation of Alkenes: Challenges and Opportunities. Angew. Chem., Int. Ed 2015, 54, 15642–15682.(d)Hu DX; Seidl FJ; Bucher C; Burns NZ, Catalytic Chemo-, Regio-, and Enantioselective Bromochlorination of Allylic Alcohols. J. Am. Chem. Soc 2015, 137, 3795–3798. [PubMed: 25738419] (e)Landry ML; Hu DX; McKenna GM; Burns NZ, Catalytic Enantioselective Dihalogenation and the Selective Synthesis of (-)-Deschloromytilipin A and (-)-Danicalipin A. J. Am. Chem. Soc 2016, 138, 5150–5158. [PubMed: 27018981] (f)Soltanzadeh B; Jaganathan A; Yi Y; Yi H; Staples RJ Borhan, B., Highly Regio- and Enantioselective Vicinal Dihalogenation of Allyl Amides. J. Am. Chem. Soc 2017, 139, 2132–2135. [PubMed: 28112919] (g)Wedek V; Van Lommel R; Daniliuc CG; De Proft F; Hennecke U Organocatalytic, Enantioselective Dichlorination of Unfunctionalized Alkenes. Angew. Chem., Int. Ed 2019, 58, 9239–9243.(h)Gilbert BB; Eey STC; Ryabchuk P; Garry O; Denmark SE, Organoselenium-catalyzed enantioselective syn-dichlorination of unbiased alkenes. Tetrahedron. 2019, 75, 4086–4098. [PubMed: 31768077]

(37). Naumann K Influence of Chlorine Substituents on Biological Activity of Chemicals: A Review. Pest Manage. Sci 2000, 56, 3–21.

(38). Bott G; Field LD; Sternhell S Steric Effects - a Study of a Rationally Designed System. J. Am. Chem. Soc 1980, 102, 5618–5626.

(39). Krautwald S; Carreira EM, Stereodivergence in Asymmetric Catalysis. J. Am. Chem. Soc 2017, 139, 5627–5639. [PubMed: 28384402]

(40). (a)Rauniyar V; Lackner AD; Hamilton GL; Toste FD Asymmetric Electrophilic Fluorination Using and Anionic Chiral Phase-Transfer Catalyst. Science 2011, 334, 1681–1684. [PubMed: 22194571] (b)Phipps RJ; Hiramatsu K; Toste FD Asymmetric Fluorination of Enamides: Access to α-Fluoroimines using an Anionic Chiral Phase-Transfer Catalyst. J. Am. Chem. Soc 2012, 134, 8376–8379. [PubMed: 22574822] (c)Wang Y-M; Wu J; Hoong C; Rauniyar V; Toste FD Enantioselective Halocyclization Using Reagents Tailored for Chiral Anion Phase-Transfer Catalysis. J. Am. Chem. Soc 2012, 134, 12928–12931. [PubMed: 22830953] (d)Shunatona HP; Früh N; Wang Y-M; Rauniyar V; Toste FD Enantioselective Fluoroamination: 1,4-Addition to Conjugated Dienes Using Anionic Phase-Transfer Catalysis. Angew. Chem., Int. Ed 2013, 52, 7724–7727.(e)Phipps RJ; Toste FD Chiral Anion Phase-Transfer Catalysis Applied to the Direct Enantioselective Fluorinative Dearomatization of Phenols. J. Am. Chem. Soc 2013, 135, 1268–1271. [PubMed: 23330962] (f)Romanov-Michailidis F; Guénée L; Alexakis A Enantioselective Organocatalytic Fluorination Induced Wagner-Meerwein Rearrangement. Angew. Chem., Int. Ed 2013, 52, 9266–9270.(g)Xie W; Jiang G; Liu H; Hu J; Pan X; Zhang H; Wan X; Lai Y; Ma D Highly Enantioselective Bromocyclization of Tryptamines and its Application in the Synthesis of (-)-Chimonanthine. Angew. Chem., Int. Ed 2013, 52, 12924–12927.(h)Wu J; Wang Y-M; Drljevic A; Rauniyar V; Phipps RJ; Toste FD A Combination of Directing Groups and Chiral Anion Phase-Transfer Catalysis for Enantioselective Fluorination of Alkenes. Proc. Natl. Acad. Sci. U.S.A 2013, 110, 13729–13733. [PubMed: 23922394] (i)Yang X; Phipps RJ; Toste FD Asymmetric Fluorination of α-Branched Cyclohexanones Enabled by a Combination of Chiral Anion Phase-Transfer Catalysis and Enamine Catalysis using Protected Amino Acids. J. Am. Chem. Soc 2014, 136, 5225–5228. [PubMed: 24684209] (j)Zi W; Wang Y-M; Toste FD An *in situ* Directing Group Strategy for Chiral Anion Phase-Transfer Fluorination of Allylic Alcohols. J. Am. Chem. Soc 2014, 136, 12864–12867. [PubMed: 25203796] (k)Shen Z; Pan X; Lai Y; Hu J; Wan X; Li X; Zhang H; Xie W Chiral Ion-Pair Organocatalyst Promotes Highly Enantioselective 2-exo Iodocyclo-etherification of Allyl Alcohols. Chem. Sci 2015, 6, 6986–6990. [PubMed: 29861937] (l)Neel AJ; Milo A; Sigman MS; Toste FD Enantiodivergent Fluorination of Allylic Alcohols: Data Set Design Reveals Structural Interplay between Achiral Directing Group and Chiral Anion. J. Am. Chem. Soc 2016, 138, 3863–3875. [PubMed: 26967114]

(41). (a)Mori K; Ichikawa Y; Kobayashi M; Shibata Y; Yamanaka M; Akiyama T Enantioselective Synthesis of Multisubstituted Biaryl Skeleton by Chiral Phosphoric Acid Catalyzed Desymmetrization/Kinetic Resolution Sequence. J. Am. Chem. Soc 2013, 135, 3964–3970. [PubMed: 23413828] (b)Mori K; Kobayashi M; Itakura T; Akiyama T Enantioselective Synthesis of Chiral Biaryl Chlorides/Iodides by a Chiral Phosphoric Acid Catalyzed Sequential Halogenation Strategy. Adv. Synth. Catal 2015, 357, 35–40.

(42). Miller E; Kim S; Gibson K; Derrick JS; Toste FD Regio- and Enantioselective Bromocyclization of Difluoroalkenes as a Strategy to Access Tetrasubstituted Difluoromethylene-Containing Stereocenters. J. Am. Chem. Soc 2020, 142, 8946–8952. [PubMed: 32352775]

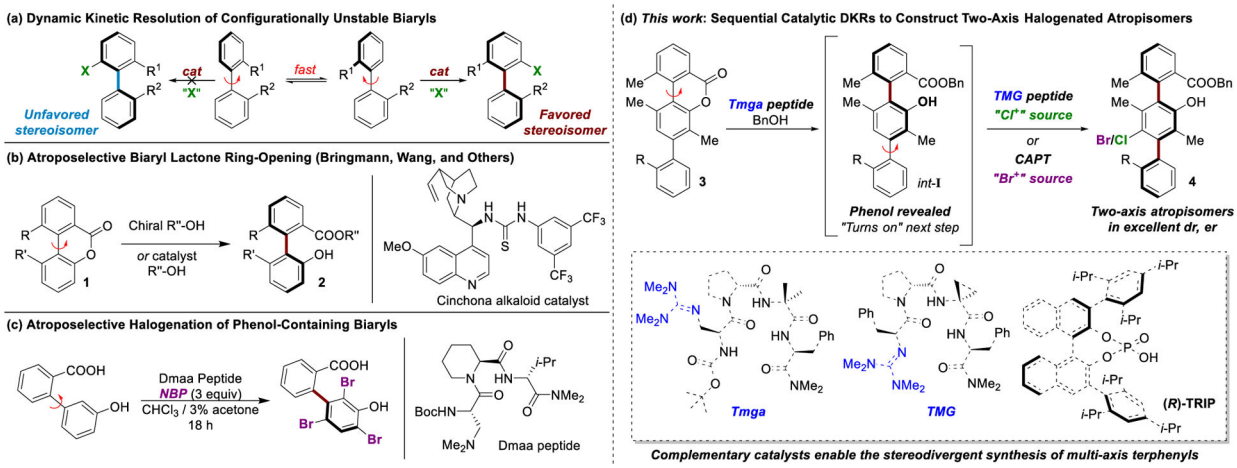

Figure 1.

(a) General scheme for the catalytic dynamic kinetic resolution of configurationally unstable biaryls, (b) Previous approaches to the DKR of biaryl lactones, (c) Peptide-catalyzed atroposelective bromination of phenol-containing biaryls, (d) Our catalytic DKR strategy to two-axis terphenyls **4** by a two-step dynamic kinetic resolution sequence.

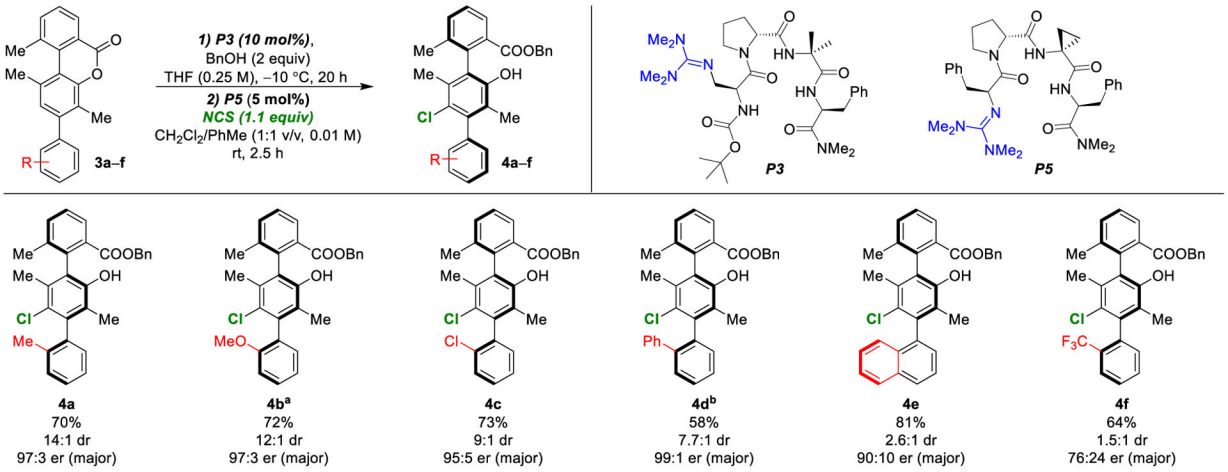

Figure 2.

Effect of bottom aryl ring substitution. Reactions are run at 0.1 mmol of lactone **3**. A short silica plug is required to remove **P3** prior to chlorination. Isolated yields, dr, and er are based off the average of two trials. Yields are reported as a mixture of diastereomers. HPLC equipped with a chiral stationary phase was used to determine dr and er. [a]Scale-up conditions were performed on 0.75 mmol (258 mg) of **3b** with the modification of portion-wise addition of NCS in the second step (see Supporting Information for experimental details). **4b** was isolated in 53% overall yield (194 mg),with 14:1 dr and 97:3 er (average of two trials). [b]2:l THF/CH_2Cl_2 solvent for ring-opening due to the poor solubility of **3d**.

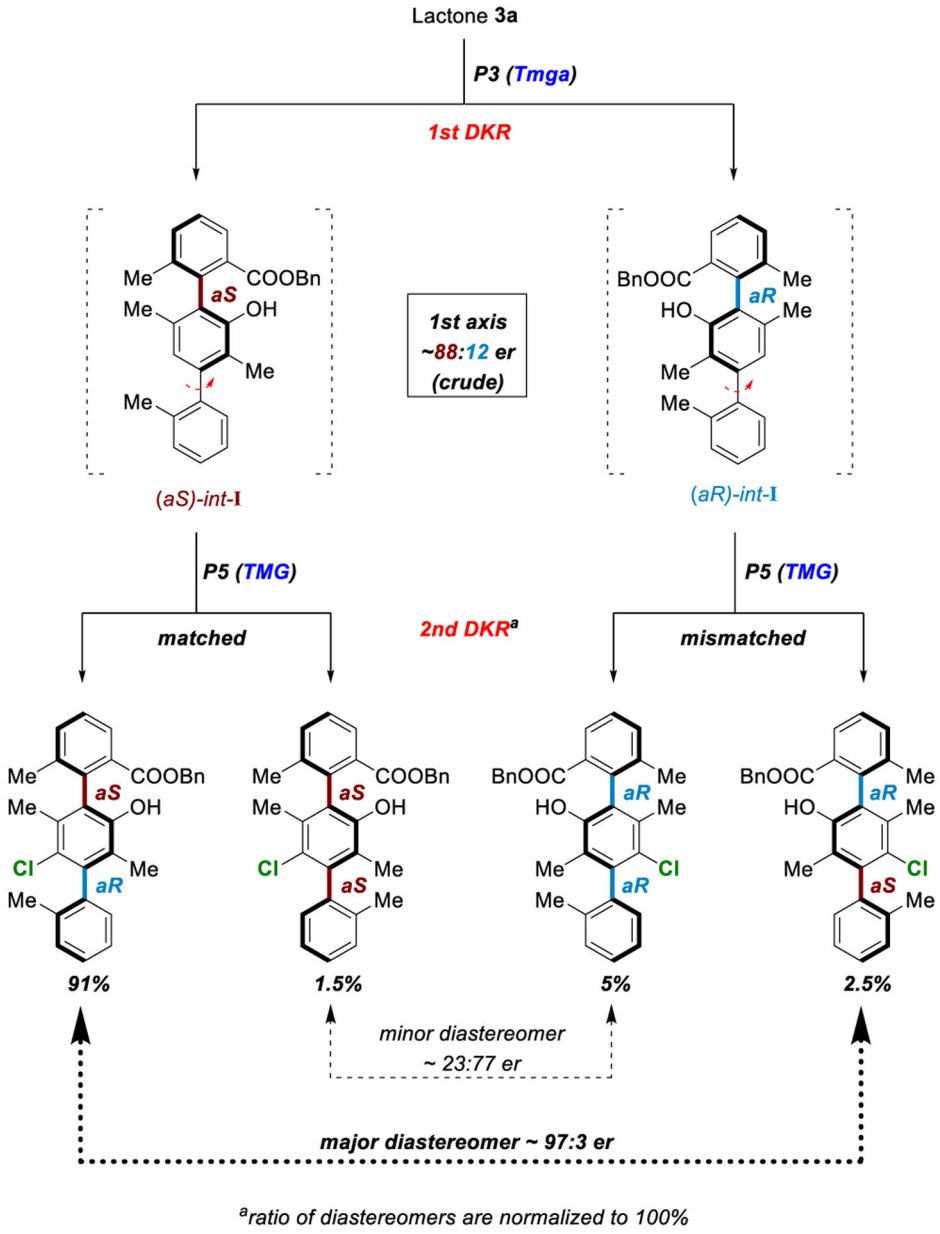

Scheme 1:
Reaction process and effects of kinetic resolution on stereoselectivity

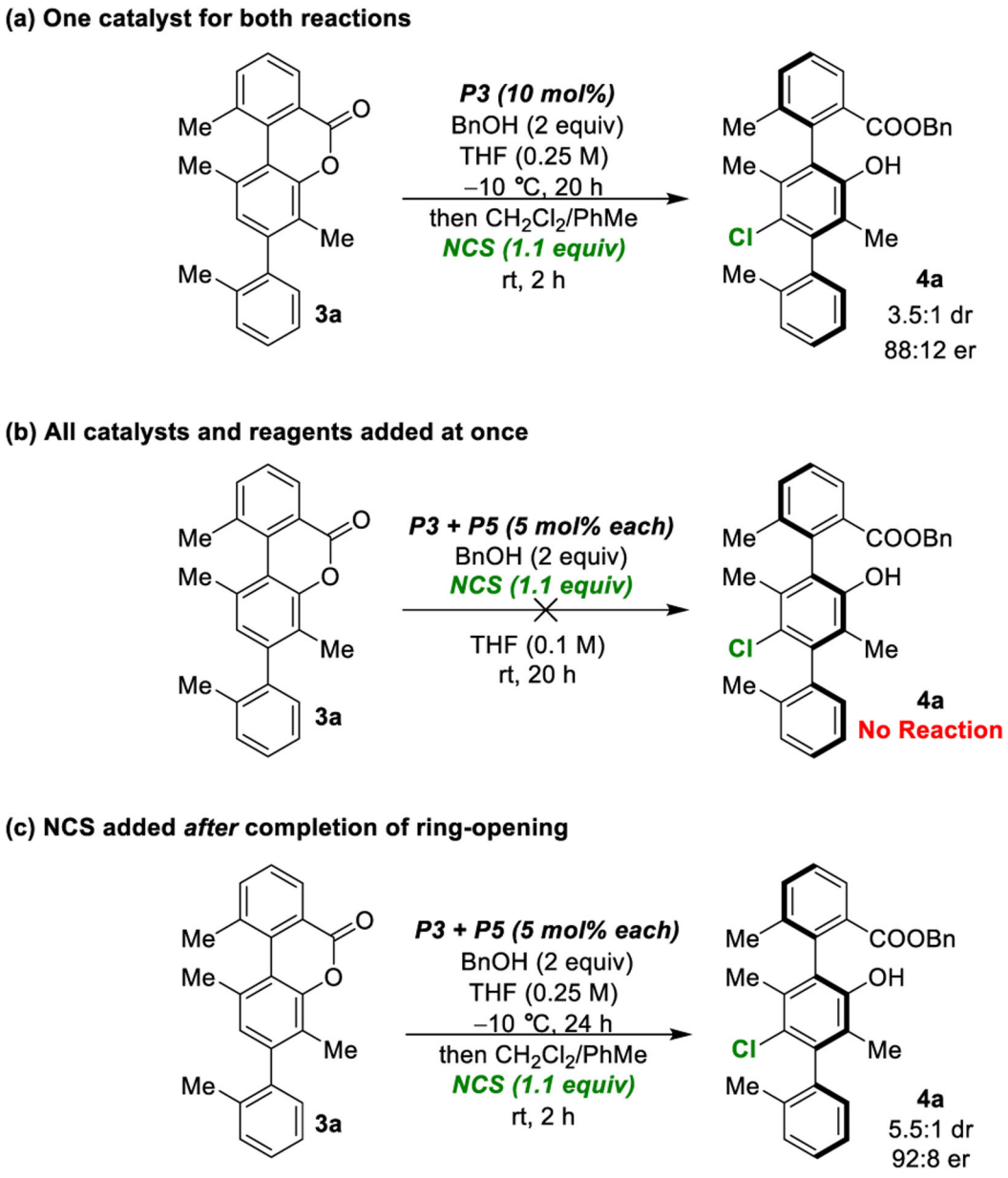

Scheme 2. Initial results towards a one-pot protocol to 4b[a]

[a]One-pot conditions: **3a** (0.1 mmol, 1.0 equiv), **P3** (5 mol%), **P5** (5 mol%) BnOH (2.0 equiv), THF (0.4 mL), −10 °C, 20 h, then CH_2Cl_2/PhMe (1:1, 9.6mL) and NCS (1.1 equiv), rt, 2 h. Reactions are run to complete conversion of **3a**. HPLC equipped with a chiral stationary phase was used to determine dr and er.

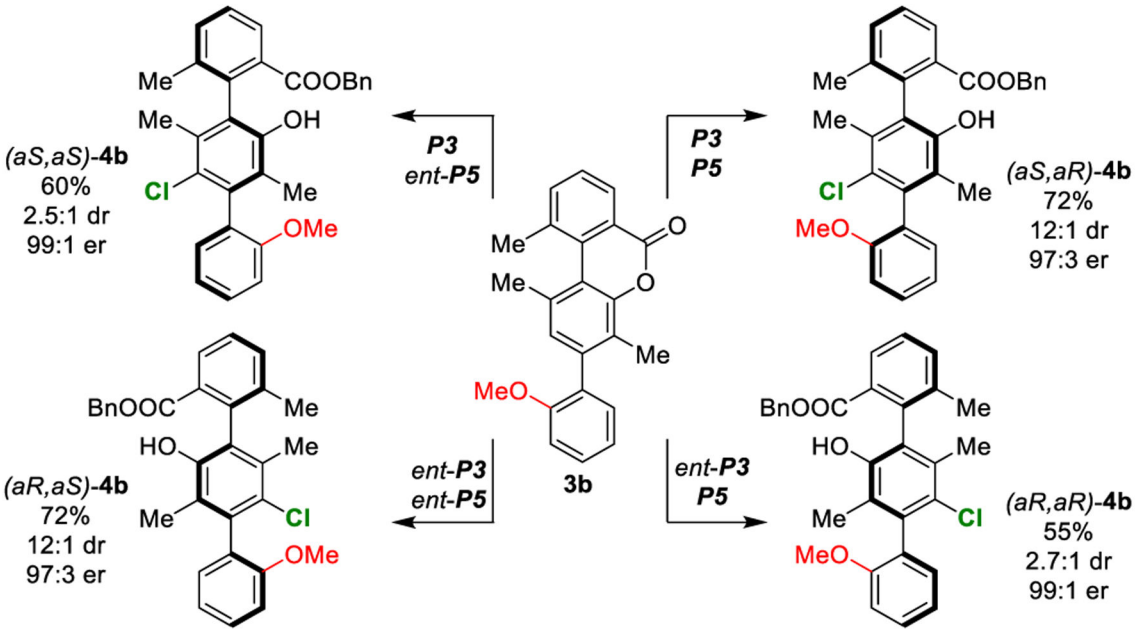

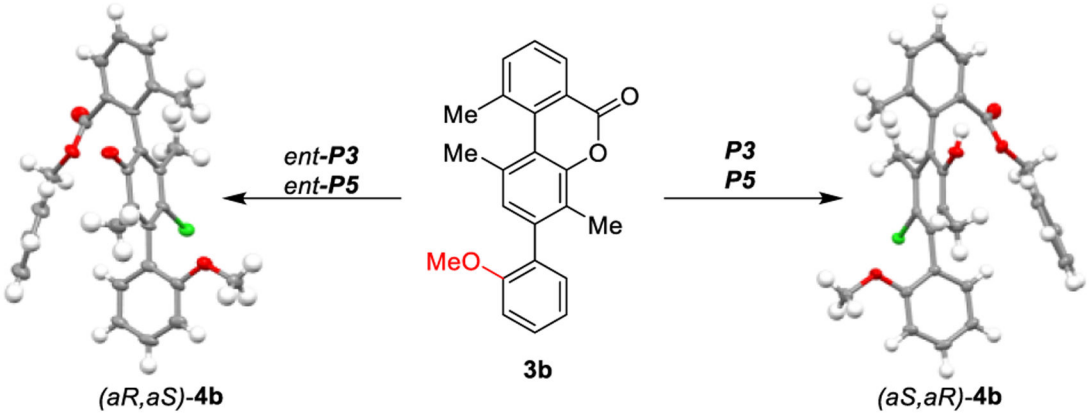

Scheme 3: Stereodivergent synthesis of all diastereomers of 4b[a]

Standard conditions: *ring-opening*. **3b** (0.1 mmol, 1.0 equiv), **P3** (10 mol%), BnOH (2.0 equiv), THF (0.4 mL), −10 °C, 20 h; *chlorination*. **P5** (5 mol%), NCS (1.1 equiv), CH_2Cl_2/PhMe (1:1 v/v, 10 mL) A short silica plug is required to remove **P3** prior to chlorination. Isolated yields, dr, and er are based off the average of two trials. Yields are reported as a mixture of diastereomers, which are separable by silica gel column chromatography. HPLC equipped with a chiral stationary phase was used to determine dr and er.

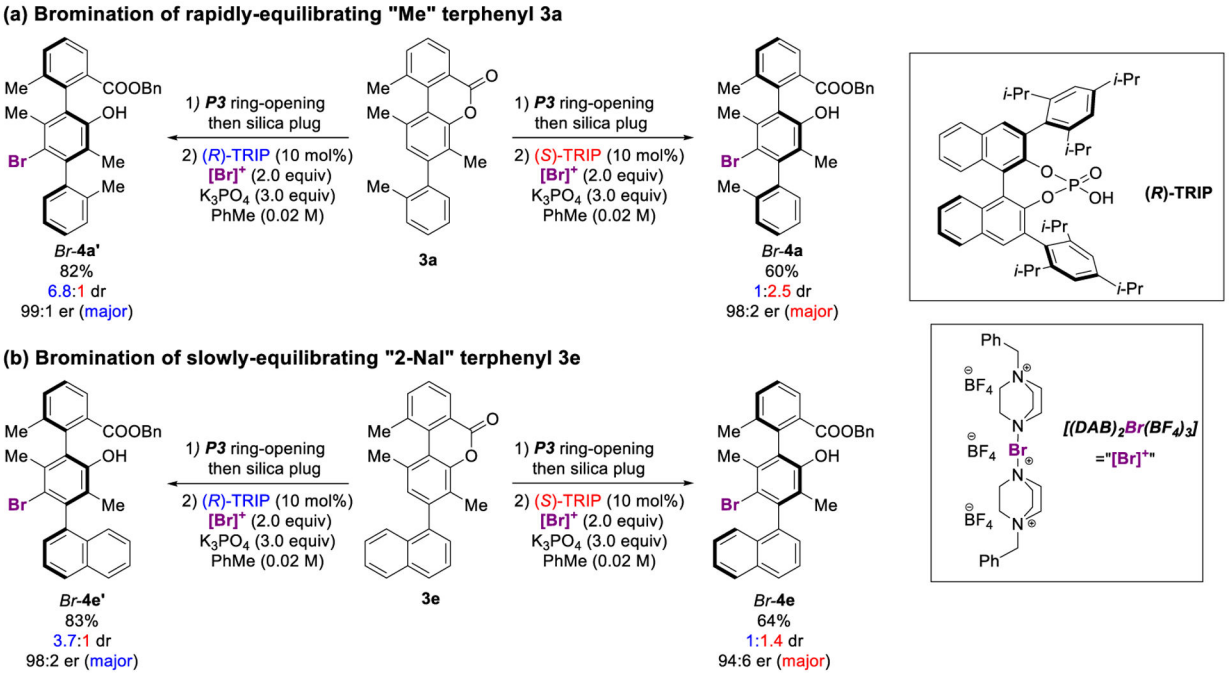

Scheme 4. Diastereodivergent Chiral Anion Phase Transfer Catalysis to Brominated Two-Axis Terphenyls

Standard conditions: *ring-opening*. **3** (0.1 mmol, 1.0 equiv), **P3** (10 mol%) BnOH (2.0 equiv), THF (0.4 ml), −10 °C, 20 h; *bromination*. TRIP (10 mol%), $[(DAB)_2Br(BF_4)_3]$ (2.0 equiv), K_3PO_4 (3.0 equiv), PhMe (5 mL), rt, 48 hours. A short silica plug is required to remove **P3** prior to bromination. Isolated yields are reported as a mixture of diastereomers. HPLC equipped with a chiral stationary phase was used to determine dr and er. We note that the stereochemical assignments for *Br*-**4a**, *Br*-**4a'**, *Br*-**4e** and *Br*-**4e'** are drawn in analogy to the X-ray based assignments of the chlorinated products, but have not been directly determined themselves (see Supporting Information for details).

Table 1:

Optimization of Atroposelective Ring-Opening

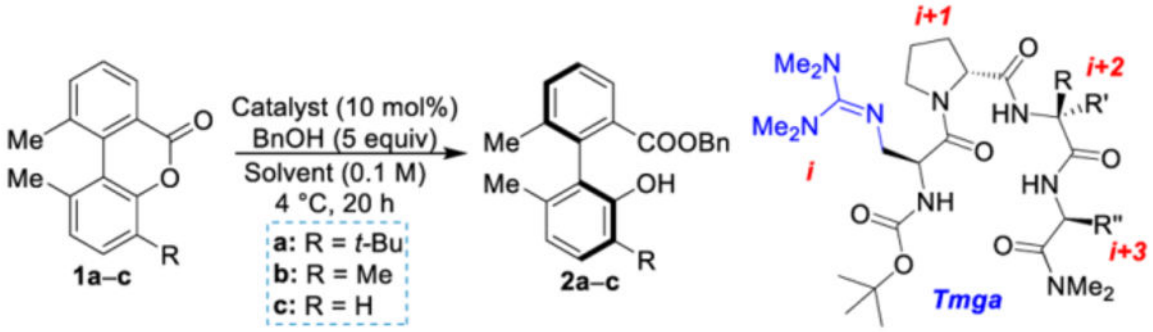

entry	"-R"	catalyst	solvent	Conv. (%)[a]	er[b]
1	**1a**	Boc-Dmaa-D-Pro-Acpc-Leu-NMe_2 (**P1**)	CH_2Cl_2	0	N/A
2	**1a**	Triethylamine	CH_2Cl_2	<5	N/A
3	**1a**	*N,N,N',N'*- tetramethylguanidine (**TMG**)	CH_2Cl_2	70	50:50
4	**1a**	Boc-Tmga-D-Pro-Aib-Leu-NMe_2 (**P2**)	CH_2Cl_2	48	74:26
5	**1a**	Boc-Tmga-D-Pro-Aib-Leu-NMe_2 (**P2**)	PhMe	62	65:35
6	**1a**	Boc-Tmga-D-Pro-Aib-Leu-NMe_2 (**P2**)	MeCN	98	83:17
7	**1a**	Boc-Tmga-D-Pro-Aib-Leu-NMe_2 (**P2**)	THF	85	87:13
8	**1a**	Boc-Tmga-D-Pro-Aib-Phe-NMe_2 (**P3**)	THF	82	91:9
9	**1a**	Boc-Tmga-D-Pro-Aib-2Nal-NMe_2 (**P4**)	THF	95	90:10
10[c]	**1a**	Boc-Tmga-D-Pro-Aib-Phe-NMe_2 (**P3**)	THF (0.25 M)	91	93:7
11[c]	**1b**	Boc-Tmga-D-Pro-Aib-Phe-NMe_2 (**P3**)	THF (0.25 M)	70	88:12
12[c]	**1c**	Boc-Tmga-D-Pro-Aib-Phe-NMe_2 (**P3**)	THF (0.25 M)	85	62:38

[a] Conversion determined by ^{1}HNMR integration ratios of product to substrate.

[b] Enantiomeric ratios determined by HPLC equipped with a chiral stationary phase.

[c] Reaction performed at −10 °C, 2 equiv BnOH. (Abbreviation: Dmaa = dimethylaminoalanine; Tmga = tetramethyl-guanidinylalanine; Aib = 2-aminoisobutyric acid; 2Nal = 3-(2-naphthyl)-alanine).

Table 2:

Optimization of Atroposelective Chlorination

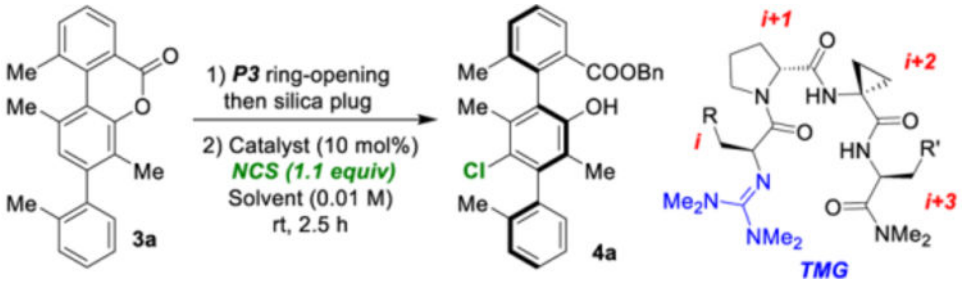

entry[a]	catalyst	solvent	dr[b]	er (maj-4a)[b]
1	No catalyst	CH_2Cl_2	N.R.	N.R.
2	Boc-Tmga-D-Pro-Aib-Phe-NMe_2 (**P3**)	CH_2Cl_2	4.6:1	88:12
3	Boc-Dmaa-D-Pro-Acpc-Leu-NMe_2 (**P1**)	CH_2Cl_2	N.R.	N.R.
4	Triazabicyclodecene (**TBD**)	CH_2Cl_2	3.9:1	88:12
5	TMG-Phe-D-Pro-Acpc-Phe-NMe_2 (**PS**)	CH_2Cl_2	13:1	92:8
6	TMG-D-Phe-D-Pro-Acpc-Phe-NMe_2 (**P6**)	CH_2Cl_2	7:1	88:12
7	TMG-Phe-Pro-Acpc-Phe-NMe_2 (**P7**)	CH_2Cl_2	5.7:1	83:17
8	TMG-Phe-D-Pro-Aib-Phe-NMe_2 (**P8**)	CH_2Cl_2	9:1	88:12
9[c]	TMG-Phe-D-Pro-Acpc-Phe-NMe_2 (**P5**)	CH_2Cl_2	9:1	94:6
10[c]	TMG-Phe-D-Pro-Acpc-Phe-NMe_2 (**P5**)	CH_2Cl_2/PhMe	14:1	97:3

[a] All reactions run to complete conversion of **3a**.

[b] Diastereomeric and enantiomeric ratios determined by HPLC equipped with a chiral stationary phase.

[c] 5 mol% catalyst loading (Abbreviations: Tmga = tetra-methylguanidinylalanine; TMG = *N,N,N′,N′*-tetramethylguanidine; Aib = 2-aminoisobutyric acid; Acpc = 1-aminocyclopropane carboxylic acid; Dmaa = dimethylaminoalanine).